nature geoscience

ARTICLES

PUBLISHED ONLINE: 22 AUGUST 2010 | DOI: 10.1038/NGEO942

# Pervasive oxygenation along late Archaean ocean margins

Brian Kendall[1]*, Christopher T. Reinhard[2], Timothy W. Lyons[2], Alan J. Kaufman[3], Simon W. Poulton[4] and Ariel D. Anbar[1,5]

**The photosynthetic production of oxygen in the oceans is thought to have begun by 2.7 billion years ago, several hundred million years before appreciable accumulation of oxygen in the atmosphere. However, the abundance and distribution of dissolved oxygen in the late Archaean oceans is poorly constrained. Here we present geochemical profiles from 2.6- to 2.5-billion-year-old black shales from the Campbellrand–Malmani carbonate platform in South Africa. We find a high abundance of rhenium and a low abundance of molybdenum, which, together with the speciation of sedimentary iron, points to the presence of dissolved oxygen in the bottom waters on the platform slope. The water depth on the slope probably reached several hundred metres, implying the export of $O_2$ below the photic zone. Our data also indicate that the mildly oxygenated surface ocean gave way to an anoxic deep ocean. We therefore suggest that the production of oxygen in the surface ocean was vigorous at this time, but was not sufficient to fully consume the deep-sea reductants. On the basis of our results and observations from the Hamersley basin in Western Australia, we conclude that the productive regions along ocean margins during the late Archaean eon were sites of substantial $O_2$ accumulation, at least 100 million years before the first significant increase in atmospheric $O_2$ concentration.**

Hydrocarbon biomarkers preserved in black shales deposited 2.7–2.5 Gyr ago may indicate the presence of small amounts of $O_2$ and $O_2$-producing cyanobacteria[1–4] in late Archaean oceans. However, an indigenous origin for these molecules has been challenged[5], and some anoxygenic photoautotrophs are also known to biosynthesize 2-methylbacteriohopanepolyols[6]. This controversy motivates the search for other geochemical evidence of biospheric $O_2$ in late Archaean sedimentary rocks. Redox-sensitive metal enrichment (rhenium (Re) and molybdenum (Mo)) and S and N isotope signatures in the Mount McRae Shale (Hamersley Basin, Pilbara Craton, Western Australia)[7–10], N isotope signatures in the Transvaal Supergroup (Griqualand West Basin, Kaapvaal Craton, South Africa)[11] and Cr isotope systematics in banded iron formations[12] (BIFs) are all consistent with the presence of $O_2$ in the late Archaean marine environment. Yet, the extent of ocean oxygenation is poorly constrained. To address this uncertainty, we obtained high-resolution geochemical profiles of Re and Mo abundances, sedimentary Fe (iron) speciation and S isotope compositions from 2.59- to 2.46-Gyr-old black shales deposited in the Griqualand West basin. In contrast to the generally deep-water 2.5-Gyr-old Mount McRae Shale, the Griqualand West shales afford an opportunity to look for geochemical evidence of water-column $O_2$ in a more proximal setting adjacent to the shelf margin of a large carbonate platform[13,14].

## Geochemical proxies for dissolved $O_2$

Re and Mo are mobilized together from upper continental crust by oxidative weathering and are transported together by rivers to the oceans as largely unreactive $ReO_4^-$ and $MoO_4^{2-}$. These metals both behave conservatively in oxygenated sea water[15–18], leading to their accumulation in the water column and a long residence time (~700–800 kyr) in the modern ocean[19]. Both Re and Mo are removed from solution to organic matter and sulphides in reducing sediments. However, their removal mechanisms are different. The accumulation rate of Re is controlled by the kinetically slow chemical reduction of $Re^{VII}$ to $Re^{IV}$ and is not tied to dissolved sulphide concentrations[20,21]. Conversely, authigenic Mo accumulation scales with sulphide availability and occurs when $MoO_4^{2-}$ reacts with sulphidic bottom or pore waters to form particle-reactive thiomolybdates ($MoO_{4-x}S_x^{2-}$) that are scavenged from solution[22–24].

The two metals are removed together from sea water in modern organic-rich sediments deposited beneath $O_2$-deficient, sulphide-bearing (euxinic) bottom waters. Strong authigenic enrichments are seen in such sediments throughout the Phanerozoic eon, where Re and Mo abundances may reach >100 ppb and >100 ppm, respectively, relative to upper crustal abundances of 1 ppb and 1–2 ppm (refs 24–27). In contrast, Re and Mo do not accumulate together when depositional conditions are less intensely reducing. In particular, when $O_2$ is present in the water column but penetrates <1 cm below the sediment/water interface, Re will accumulate, but Mo sequestration is limited by low sulphide concentrations in pore waters. Under such conditions, high Re but minimal Mo enrichments are observed in sediments in modern continental margin environments[19,25,28]. Comparison of Re and Mo abundances therefore provides a sensitive measure of ancient water-column redox conditions.

An absence of Re and Mo enrichment in sediments may indicate an oxygenated water column ($O_2$ penetration depths of >1 cm; refs 19,25,28) or negligible oxidative weathering beneath an $O_2$-poor atmosphere and thus very small amounts of dissolved Re and Mo in sea water. In view of this ambiguity, we turn to an independent proxy for water-column redox conditions, specifically sedimentary Fe speciation. In modern sediments deposited from

[1]School of Earth and Space Exploration, Arizona State University, Tempe, Arizona 85287, USA, [2]Department of Earth Sciences, University of California, Riverside, California 92521, USA, [3]Department of Geology and Earth System Science Interdisciplinary Center, University of Maryland, College Park, Maryland 20742, USA, [4]School of Civil Engineering and Geosciences, Newcastle University, Drummond Building, Newcastle upon Tyne NE1 7RU, UK, [5]Department of Chemistry and Biochemistry, Arizona State University, Tempe, Arizona 85287, USA. *e-mail: brian.kendall@asu.edu.

anoxic bottom waters, the ratio of highly reactive Fe to total Fe ($Fe_{HR}/Fe_T$) is higher (typically >0.38) compared with modern (average = 0.26 ± 0.08) and Phanerozoic (average = 0.14 ± 0.08) sediments deposited from oxygenated waters[29–31]. Hence, low values of $Fe_{HR}/Fe_T$ and negligible Re and Mo enrichment in sediments together indicate an oxygenated water column.

## Pervasive oxygenation along a late Archaean ocean margin

The Campbellrand–Malmani platform represents one of Earth's oldest and best preserved carbonate platforms, which probably extended over >600,000 km$^2$ adjacent to a large ocean basin[32] (Fig. 1). We obtained high-resolution geochemical profiles from black shales (average total organic carbon (TOC) content of 3 weight% (wt%)) of the upper Nauga and Klein Naute Formations (see Supplementary Table S1 and the Methods section). Samples were obtained from two drill cores located 24 km apart on the slope of the carbonate platform. At these localities, the carbonate-dominated upper Nauga Formation contains black shale beds up to 20 m thick. Two of these shale beds are stratigraphically correlative (N1 at 637–641 m in GKP01 and 829–839 m in GKF01; N2 at 483–496 m in GKP01 and 616–627 m in GKF01); the uppermost shale bed in GKF01 (N3 at 440–455 m) is not found in GKP01 (Supplementary Fig. S1; ref. 13). Drowning of the carbonate platform resulted in progressively deeper-water deposition of pyritic black shales and cherts of the overlying Klein Naute Formation, followed by the Kuruman BIF (refs 13,32–34). U–Pb zircon dating of volcanic tuff beds indicates the black shales were deposited between 2,588 ± 6 and 2,460 ± 5 Myr ago[14,35,36].

Compelling geochemical evidence of mild but pervasive oxygenation of the surface ocean along the Campbellrand–Malmani margin comes from the Nauga N2 and N3 shales. In both cores, these shales have strong enrichment in Re (Al-normalized enrichment factor (EF) = 4–40) but negligible Mo enrichment (EF < 2) (Figs 2, 3). By analogy with modern environments characterized by these distinctive relative enrichments, we infer that Re, Mo and small amounts of dissolved $O_2$ were all present in bottom waters on the slope beneath the Campbellrand–Malmani carbonate platform. On the basis of the typical range of $O_2$ contents in such modern environments, local bottom-water $O_2$ concentrations of <10–100 μM are indicated[19,25,28]. However, further calibration of this proxy is needed to determine if the $O_2$ concentrations observed in the modern environments can be straightforwardly extrapolated to the late Archaean. The alternative possibility that the sediments reflect late Archaean sea water with high Re but low Mo concentrations is unlikely because these metals reside together in sulphide minerals and organic matter in crustal rocks and therefore should undergo simultaneous oxidative mobilization and enter sea water together. Other alternative explanations for the juxtaposition of high Re and negligible Mo enrichment in shales are not known.

Further evidence of oxygenation comes from N1 in both cores, which feature negligible Re and Mo enrichment (EF < 3). These low Re and Mo abundances could reflect negligible oxidative weathering and the absence of these metals in the water column. However, we find that the shales with negligible Re and Mo enrichment also exhibit low $Fe_{HR}/Fe_T$ values (average = 0.22 ± 0.11). These low values are similar to modern and Phanerozoic sediments deposited from oxygenated waters, suggesting that the bottom waters at both localities were sufficiently oxygenated to prevent accumulation of Re and Mo in the sediments despite their availability in the water column.

As water depths on the slope probably reached several hundred metres[14,33] (see Fig. 1), the Mo, Re and Fe data imply the presence of $O_2$ below the photic zone. It is difficult to account for $O_2$ at such depths without invoking pervasive oxygenation of the overlying surface ocean. That scenario, in turn, points to cyanobacterial oxygenic photosynthesis to provide the large quantities of $O_2$ required for mild oxygenation of the water column on the platform slope. As the Nauga Formation shales were deposited at or before 2,560 ± 6 Myr ago[14], we conclude that substantial $O_2$ accumulation occurred along this productive ocean margin more than 100 Myr before the first major increase in atmospheric $O_2$ (Great Oxidation Event (GOE); refs 37,38).

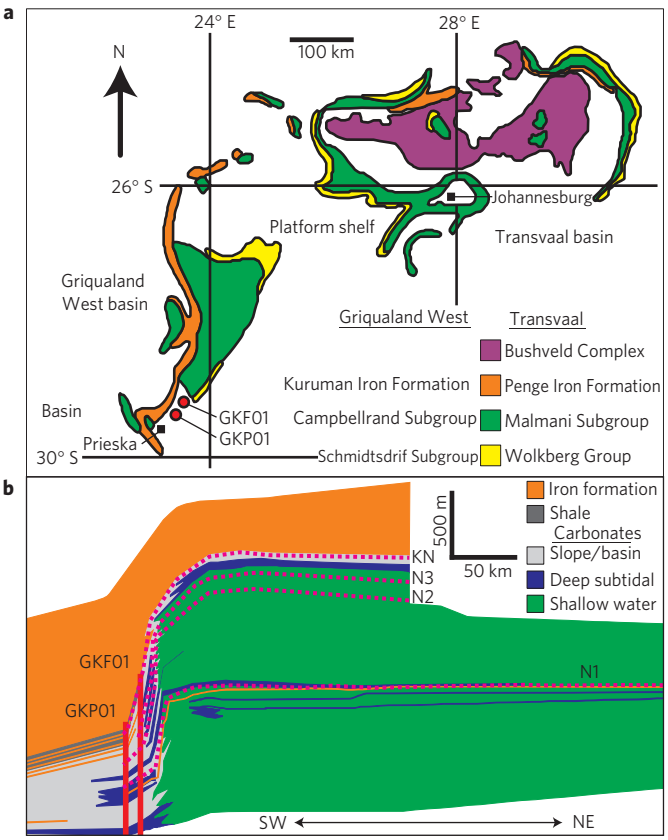


**Figure 1 | Geological map and cross-section of the Campbellrand–Malmani carbonate platform margin. a**, Map showing exposures of the 2.67- to 2.46-Gyr-old succession of the Transvaal Supergroup (Kaapvaal craton, South Africa) and the location of the two cores GKP01 and GKF01 (ref. 33). **b**, Simplified cross-section from southwest to northeast across the Griqualand West basin. The dashed pink lines trace the stratigraphic position of the black shale intervals from the cores onto the platform shelf, as inferred from sequence stratigraphy[14,33]. The palaeobathymetry along the slope is difficult to determine precisely and is probably exaggerated. Nauga Formation: N1 = 637–641 m in GKP01 and 829–839 m in GKF01; N2 = 483–496 m in GKP01 and 616–627 m in GKF01; N3 = 440–455 m in GKF01. Klein Naute Formation: KN.

## Redox stratification of the late Archaean ocean margins

In contrast to the fully oxygenated modern oceans, however, the oxic surface waters along late Archaean ocean margins gave way to anoxic deep and open ocean waters. In the N2 and N3 shale beds, which may have been deposited at water depths greater than those of N1 (see Fig. 1), low $Fe_{HR}/Fe_T$ ratios (average = 0.26 ± 0.06) in the more proximal core (GKF01) imply oxygenated bottom waters, consistent with the high Re and low Mo enrichments. In contrast, higher $Fe_{HR}/Fe_T$ ratios (average = 0.40 ± 0.10) are observed from N2 in the more distal core (GKP01) but, uncharacteristically, also with high Re and low Mo enrichments. Mixed redox signatures are expected in a transitional setting, so we suggest that the episodic excursions to higher $Fe_{HR}/Fe_T$ in N2 from GKP01 may reflect intermittent anoxia or precipitation of dissolved Fe(II) upwelled from deeper anoxic waters onto the mildly oxygenated sea floor.

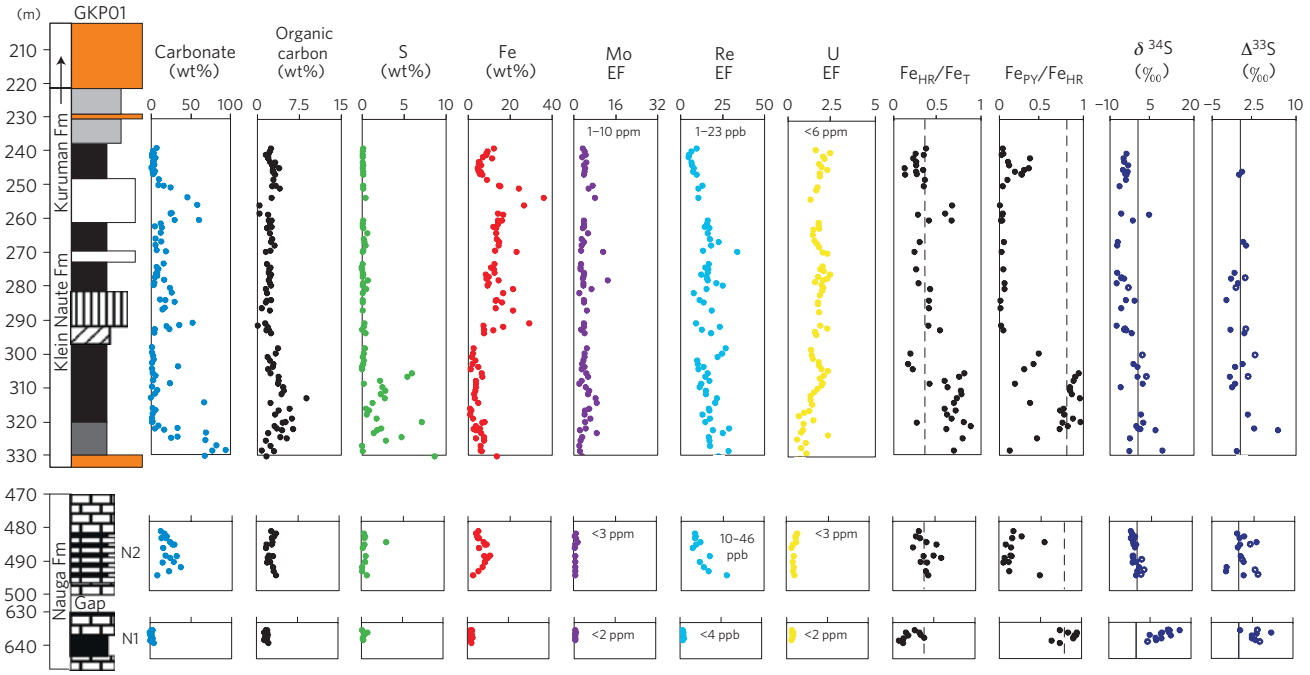


**Figure 2 | Geochemical profiles through core GKP01.** Enrichment factor (EF) = $(metal/Al)_{sample}/(metal/Al)_{average\ upper\ crust}$. Total Fe, highly reactive Fe and pyrite Fe are denoted by $Fe_T$, $Fe_{HR}$ and $Fe_{PY}$, respectively. The open circles in the S isotope profiles are from ref. 47. For an anoxic water column ($Fe_{HR}/Fe_T$ typically >0.38), $Fe_{PY}/Fe_{HR}$ distinguishes between euxinic (>0.8) and ferruginous (<0.8) conditions. High $Fe_{PY}/Fe_{HR}$ and low $Fe_{HR}/Fe_T$ (for example, N1 shale beds) reflects microbial $H_2S$ production within sediments and extensive sulphidation of available $Fe_{HR}$, but minimal enrichment of $Fe_{HR}$ in sediments underlying an oxic water column. Stratigraphic column legend: orange =banded iron formation/chert; white = chert with thin shale/carbonate; light grey = chert/shale; vertical rule = chert/carbonate; bricks = carbonate; diagonal rule = carbonate/shale; dark grey = carbonate-rich base transitioning to dolomitic, organic-rich shale; black = black shale.

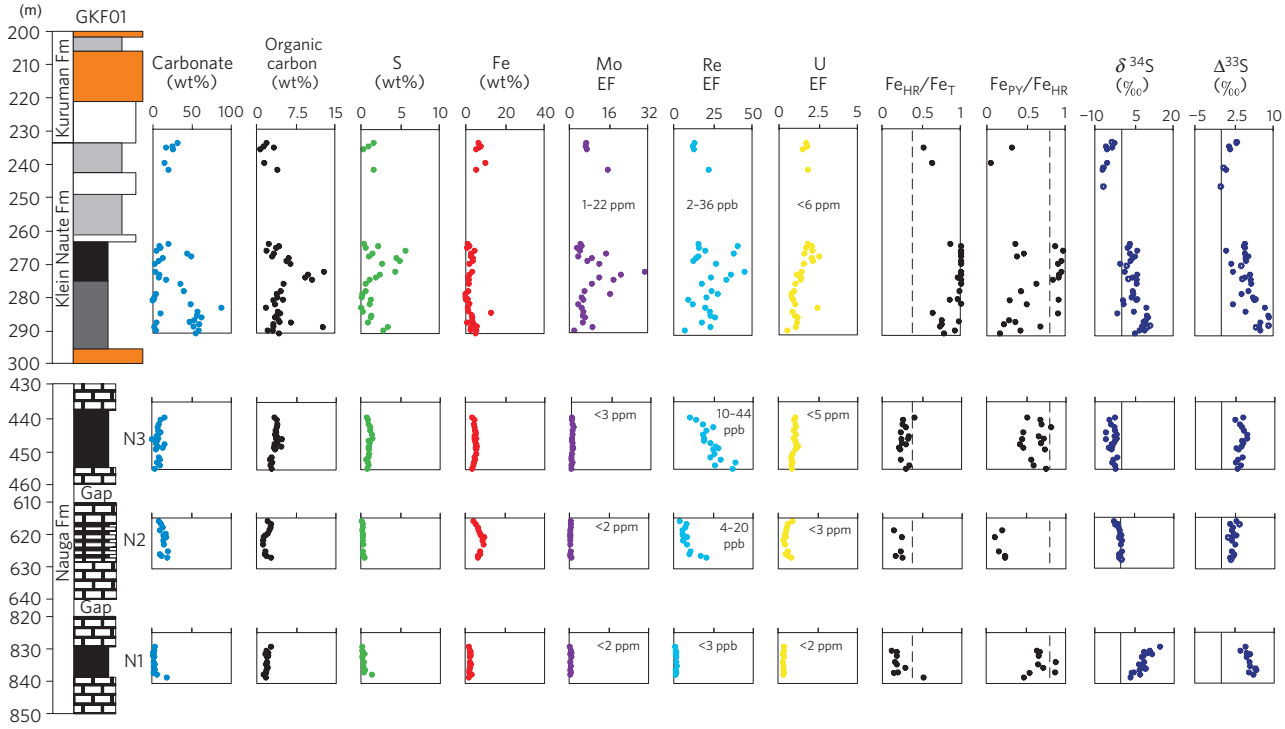


**Figure 3 | Geochemical profiles through core GKF01.** The abbreviations and legend are defined in Fig. 2.

Hence, water depths at this site were probably proximal to the chemocline (Fig. 4). Given water depths of chemoclines in modern anoxic marine basins, we suggest the chemocline was located up to a few hundred metres below the photic zone at the GKP01 locality[24].

Geochemical data from the Klein Naute Formation constrain the redox state of deeper waters after the carbonate platform drowned. In the lower Klein Naute Formation in both cores, $Fe_{HR}/Fe_T$ is consistently high (>0.38), pointing to anoxic conditions. The high

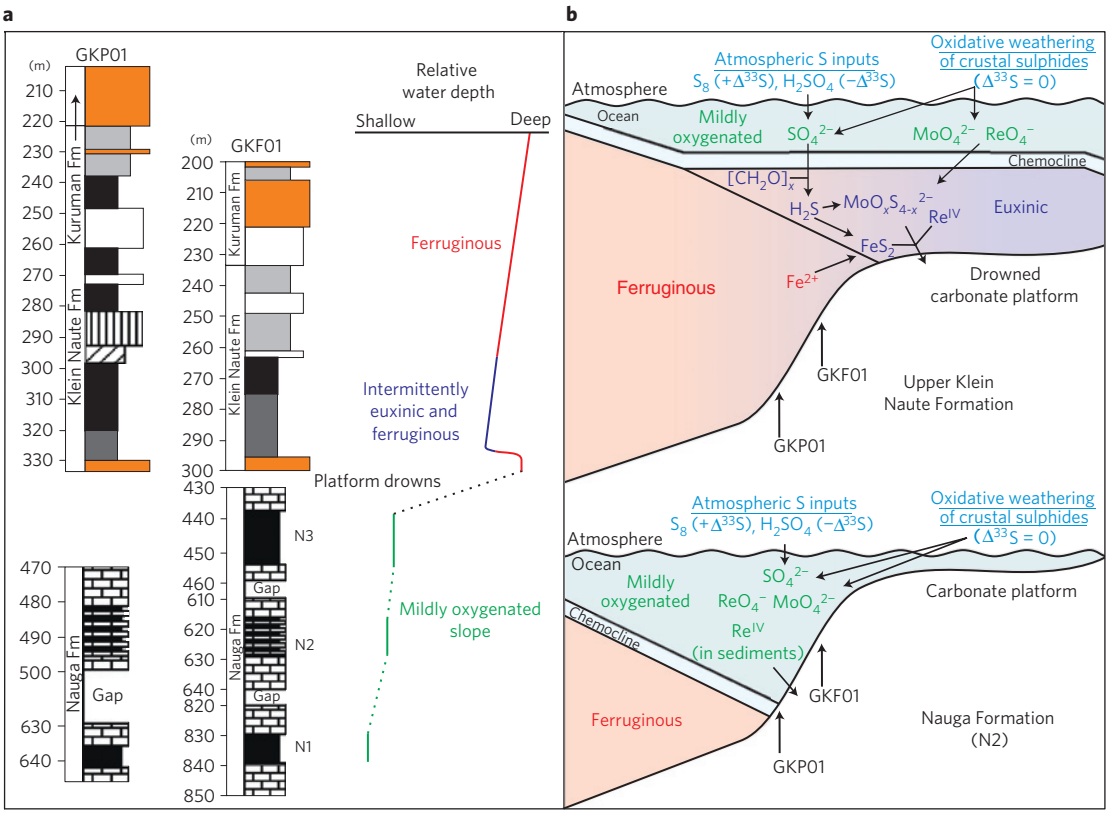


**Figure 4 | Late Archaean ocean redox conditions along the Campbellrand–Malmani ocean margin. a**, Simplified relative water-depth profile. **b**, Ocean redox conditions on the platform and slope. $O_2$ accumulation was confined to the shallow waters (up to several hundred metres) along the ocean margin where rates of photosynthetic $O_2$ production were high. At mid-water depths, locally high organic carbon and sulphate fluxes promoted extensive microbial $H_2S$ production, leading to euxinic conditions. Otherwise, the deep (and open) ocean was anoxic and ferruginous. During upper Nauga time, the water column on the platform slope was mildly oxygenated, but drowning of the carbonate platform (Klein Naute Formation) resulted in replacement of the oxic waters with deeper anoxic waters. The low-$O_2$ atmosphere permitted both mass-independent fractionation of S isotopes and oxidative mobilization of sulphate, Re and Mo from weathering of crustal sulphide minerals.

$Fe_{HR}/Fe_T$ is associated with episodes of higher (>0.8) and lower (<0.8) ratios of $Fe_{PY}/Fe_{HR}$, which indicate euxinic and ferruginous water columns, respectively[10,29,39]. Euxinic conditions arise when organic carbon and sulphate fluxes are sufficiently high for extensive microbial production of $H_2S$, which then quantitatively titrates $Fe^{2+}$ from the water column through sedimentary pyrite formation. The low $Fe_{PY}/Fe_{HR}$ values (typically near 0), high $Fe_T$ abundances (commonly >10 wt%) and elevated $Fe_{HR}/Fe_T$ in the upper Klein Naute Formation, together with deposition of the overlying Kuruman BIF, are strong indicators that the late Archaean deep ocean was anoxic and ferruginous[10,39,40]. Some $Fe_{HR}/Fe_T$ values in this interval are relatively low (<0.38), but the high $Fe_T$ abundances are not consistent with oxic conditions. Instead, the low $Fe_{HR}/Fe_T$ values may result from the incorporation of unsulphidized, reactive Fe into poorly reactive silicates during diagenesis or metamorphism (and not included in the $Fe_{HR}$ pool) or from incomplete extraction of crystalline siderite in some Fe-rich samples[10,41]. We interpret these data in a sequence stratigraphic context and propose that the mildly oxygenated slope environment was replaced by anoxic deeper waters after the platform drowned (see Fig. 4). The episodic excursions to higher and lower $Fe_{PY}/Fe_{HR}$ in the lower Klein Naute Formation may capture a metastable zone of mid-water-column euxinia within the ferruginous deep ocean[10,42].

## Oxidative weathering on the late Archaean Earth

During lower Klein Naute time, the episodes of water-column euxinia would have permitted both Mo and Re accumulation in sediments. In the GKF01 core, a distinctive peak in Mo and TOC abundance occurs in the predominantly euxinic interval between 275 and 268 m. In contrast, a similar peak in Mo enrichment is not observed in the more distal GKP01 core despite Fe speciation evidence for euxinia at 320–305 m. Average Mo/TOC ratios, which scale with Mo concentrations in sulphidic bottom waters[24], are ~2 and ~1 ppm per wt% in the euxinic GKF01 and GKP01 intervals, respectively. Re/TOC relationships are less straightforward[26,43], but Re enrichment in GKF01 also generally exceeds that in GKP01. We infer that water-column Mo and Re inventories were larger in shallower relative to deeper waters on the drowned platform slope. In addition, the Mo/TOC ratios are small compared with Proterozoic and Phanerozoic euxinic shales (average of 6 and 27 ppm per wt%, respectively)[27]. Collectively, these observations suggest that Mo and Re entered the oceans largely from continental sources and that the oceanic residence times of these metals were short. These are the expected consequences if oxidative weathering delivered Mo and Re to predominantly anoxic oceans.

Mass-independent fractionation of S isotopes ($\Delta^{33}S \neq 0‰$) in the Nauga and Klein Naute Formations and the Mount McRae Shale indicates that atmospheric $pO_2$ was <0.001% of the present atmospheric level[8,10,44–47] (PAL). Previous studies have suggested that subaerial and/or submarine oxidative weathering of crustal sulphides can occur at such low $pO_2$ levels[7,10]. At $pO_2 = 0.001\%$ PAL, complete abiotic oxidation and dissolution of fine-grained pyrite crystals from igneous rocks in subaerial environments can occur in tens of thousands of years, although microbial processes probably enabled more rapid dissolution kinetics[7,10]. This timescale is small compared with the likely million-year or

multi-million-year duration of the shale intervals as inferred from average sedimentation rates[33,35]. Alternative anaerobic oxidants such as $Fe^{3+}$ from anoxygenic photosynthesis are less likely because the acidity from late Archean rain water and sulphide oxidation would have been unfavourable for anoxygenic photoautotrophs[10]. Models of late Archaean weathering suggest that subaerial oxidation of $MoS_2$ and $ReS_2$ could occur near regions of photosynthetic oxygen production in the adjacent shallow ocean[48]. In contrast, uraninite was not oxidized. Instead of sulphides, U in crustal rocks is primarily hosted by feldspars, zircon, apatite and sphene, which are less susceptible to oxidation at low $pO_2$. Hence, the low U abundances in late Archaean shales from the Griqualand West and Hamersley basins are consistent with limited oxidative mobilization of uranium[7].

## Implications for the chronology of biospheric oxygenation

A clearer picture of biospheric oxygen distributions on the late Archaean Earth is beginning to emerge. Combined with previous results from the Mount McRae Shale[7–10], our data indicate that surface ocean oxygenation was widespread on late Archaean ocean margins. Palaeomagnetic reconstructions suggest that our cores from the Griqualand West and Hamersley basins were ~1,000 km apart, even if the two basins faced the same ocean as part of the hypothesized continent Vaalbara[14,49]. Broad temporal correlation between the Mount McRae Shale and Klein Naute Formation is suggested by geochronological constraints[7,14,35,36], the presence of identical impact ejecta layers in overlying BIF (ref. 50) and similar $\Delta^{33}S$ and $\delta^{34}S$ signatures[8,10,47] (Supplementary Fig. S2). In particular, the wide range in $\Delta^{33}S$ (up to +10‰) from shales in the lower part of both formations contrasts with the smaller $\Delta^{33}S$ (typically $0 \pm 2$‰) in the overlying shales and BIFs (refs 8, 10,46,47). We interpret this change to reflect a small increase in atmospheric $pO_2$ at ~2.50 Gyr that preceded the GOE (refs 7,8,10). The GOE is marked by the disappearance of mass-independent fractionation of S isotopes ($\Delta^{33}S = 0.0 \pm 0.3$‰) between 2.45 and 2.32 Gyr ago in sedimentary rocks overlying Kuruman-equivalent BIFs ($pO_2 > 0.001\%$ PAL; refs 37,38,44,45).

We hypothesize that $O_2$ accumulation was widespread in productive regions along late Archaean ocean margins. Given that the studied cores reflect ocean margin environments, it remains unknown whether the open surface ocean away from the continents contained trace amounts of $O_2$ or was fully anoxic. Appreciable accumulation of atmospheric $O_2$ did not occur at this time because the rate of photosynthetic $O_2$ production was not sufficient to overcome $O_2$ consumption by crustal weathering or by reaction with reduced gases in the atmosphere and the anoxic deep oceans. We propose, then, that the late Archaean eon represents a new intermediate stage in Earth surface oxygenation.

## Methods

**Trace metals.** Sample powder preparation, dissolution and trace-metal analysis were carried out at the W. M. Keck Foundation Laboratory for Environmental Biogeochemistry, Arizona State University. Samples were broken into chips without metal contact and then ground to fine powder in a silicon nitride ball mill. Approximately 75–80 mg of sample powder was ashed at 550 °C overnight, and dissolved in 5 ml concentrated $HNO_3$ and 1 ml concentrated HF at ~150 °C for ~10 h, followed by 2 ml concentrated HCl for ~10 h. As a result of variations in sample composition, further acid attacks (usually aqua regia) were sometimes necessary to achieve complete dissolution. Sample solutions were then diluted 400-fold (only Re) or 4,000–5,000-fold (other metals) by 2% $HNO_3$, with trace HF added to ensure sample stability. Metal abundances were measured by quadrupole inductively coupled plasma mass spectrometry using multiple element calibration standards designed to have similar concentrations to organic-rich shales. Elements Ge, In, Y and Bi were used as internal standards to correct for signal drift. Secondary standards were run multiple times during each analytical session to verify instrument accuracy. Re accuracy was verified by analysis of black shale digests with Re concentrations that were independently known by isotope-dilution negative thermal ionization mass spectrometry. Measurement accuracy of other metals was verified by analysis of the US Geological Survey Devonian black shale standard SDO-1. Analyte concentration reproducibility was typically better than 5%. For samples with low Re abundances (<3 ppb), reproducibility degrades to 5–15%.

**Sedimentary Fe speciation.** Fe speciation analyses were carried out at the Department of Earth Sciences, University of California, Riverside. The speciation of highly reactive iron ($Fe_{HR}$), which comprises pyrite iron and other iron phases that will react with sulphide to form pyrite in the water column or during early diagenesis, was obtained using a calibrated sequential extraction protocol[10]. Roughly 100 mg of sample powder was first treated with a buffered sodium acetate solution (pH = 4.5), which extracts carbonate-associated Fe (either siderite, ferroan calcite or dolomite-ankerite solid-solution series). This fraction is here referred to as $Fe_{Carb}$. Samples were then treated with a sodium dithionite solution (50 g $l^{-1}$) buffered to pH = 4.8 with acetic acid and sodium citrate. Fe obtained from this extraction step, here referred to as $Fe_{Ox}$, consists of 'reducible' iron oxide phases, or iron oxides such as goethite and haematite that are reactive to hydrogen sulphide on early diagenetic timescales. Magnetite ($Fe_{Mag}$), a mixed-valence iron oxide that does not react with dithionite, was extracted with a 0.2 M ammonium oxalate and 0.17 M oxalic acid solution (pH = 3.2). Sequential extracts were analysed on an Agilent 7500ce inductively coupled plasma mass spectrometer after 100-fold dilution of extracts in trace-metal grade 2% $HNO_3$. Analytical reproducibility was typically better than ~4%, with the exception of some low-Fe samples (primarily dithionite extracts) where analytical reproducibility was ~7–12%. Pyrite iron ($Fe_{PY}$)was calculated (assuming a stoichiometry of $FeS_2$) based on wt% sulphur extracted during a 2 h hot chromium chloride distillation followed by iodometric titration. Analytical reproducibility varied between less than 1% and 6%, but was typically below ~3%. Highly reactive iron is defined as $Fe_{HR} = Fe_{Carb} + Fe_{Ox} + Fe_{Mag} + Fe_{PY}$.

**Carbonate, sulphur and TOC abundances.** Total C and S and total inorganic carbon (TIC) abundances were determined at the Institute of Geology and Paleontology, University of Muenster, Germany. Total C and S abundances were determined by offline combustion of powdered samples and analysis on a Ströhlein Instruments CS-Mat 5500. For wt% carbonate and wt% TIC determinations, sample powders were acidified with 6 M HCl, washed with Milli-Q water and dried overnight. The wt% carbonate in the sample was calculated as follows: (original sample weight − sample weight following acidification)/original sample weight ×100. The wt% TIC was determined by multiplying wt% carbonate by ~0.12. TOC was determined from the difference between total C and TIC.

**Sulphur isotopes.** S isotope analyses were carried out at the Isotope Geochemistry Laboratory, Department of Geology, University of Maryland, using an online Eurovector elemental analyser interfaced with a GV IsoPrime isotope ratio mass spectrometer[8] (IRMS). After acidification to remove carbonate, equal amounts of sample and $V_2O_5$ are folded into tin cups that are dropped sequentially into a catalytic combustion furnace ($T$ = 1,030 °C) along with a pulsed $O_2$ purge of 12 ml. Quantitative oxidation and $O_2$ resorption is accomplished in a quartz reaction tube packed with reduced copper wire. A 10 cm magnesium perchlorate column is used to remove water following combustion. SO separation is carried out in a 0.8 m polytetrafluoroethylene gas chromatography column (Porapak 50–80 mesh, $T$ = 90 °C) and purified SO is introduced to the IsoPrime IRMS along with He (80–120 ml $min^{-1}$). At the beginning of the sample run, timed pulses of SO reference gas (Air Products 99.9% purity, ~3 nA) are bled into the IRMS. S isotope ratios of the sample and reference peaks are determined by comparison of integrated peak areas of $m/z$ 48, 49 and 50 relative to baseline. Reported $\delta^{34}S$ and $\Delta^{33}S$ values are averages of triplicate measurements, which have 1$\sigma$ uncertainties typically better than 0.3‰. Comparable uncertainties are obtained from multiple measurements (~15–20) of the NBS-127 standard during each analytical session.

Received 18 February 2010; accepted 26 July 2010; published online 22 August 2010

## References

1. Brocks, J. J., Logan, G. A., Buick, R. & Summons, R. E. Archean molecular fossils and the early rise of eukaryotes. *Science* **285,** 1033–1036 (1999).
2. Summons, R. E., Jahnke, L. L., Hope, J. M. & Logan, G. M. 2-methylhopanoids as biomarkers for cyanobacterial oxygenic photosynthesis. *Nature* **400,** 554–557 (1999).
3. Brocks, J. J., Buick, R., Summons, R. E. & Logan, G. A. A reconstruction of Archean biological diversity based on molecular fossils from the 2.78 to 2.45 billion-year old Mount Bruce Supergroup, Hamersley Basin, Western Australia. *Geochim. Cosmochim. Acta* **67,** 4321–4335 (2003).
4. Waldbauer, J. R., Sherman, L. S., Sumner, D. Y. & Summons, R. E. Late Archean molecular fossils from the Transvaal Supergroup record the antiquity of microbial diversity and aerobiosis. *Precambr. Res.* **169,** 28–47 (2009).
5. Rasmussen, B., Fletcher, I. R., Brocks, J. J. & Kilburn, M. R. Reassessing the first appearance of eukaryotes and cyanobacteria. *Nature* **455,** 1101–1104 (2008).

6. Rashby, S. E., Sessions, A. L., Summons, R. E. & Newman, D. K. Biosynthesis of 2-methylbacteriohopanepolyols by an anoxygenic phototroph. *Proc. Natl Acad. Sci.* **104,** 15099–15104 (2007).
7. Anbar, A. D. *et al.* A whiff of oxygen before the great oxidation event? *Science* **317,** 1903–1906 (2007).
8. Kaufman, A. J. *et al.* Late Archean biospheric oxygenation and atmospheric evolution. *Science* **317,** 1900–1903 (2007).
9. Garvin, J. *et al.* Isotopic evidence for an aerobic nitrogen cycle in the Latest Archean. *Science* **323,** 1045–1048 (2009).
10. Reinhard, C. *et al.* A Late Archean sulfidic sea stimulated by early oxidative weathering of the continents. *Science* **326,** 713–716 (2009).
11. Godfrey, L. V. & Falkowski, P. G. The cycling and redox state of nitrogen in the Archaean ocean. *Nature Geosci.* **2,** 725–729 (2009).
12. Frei, R., Gaucher, C., Poulton, S. W. & Canfield, D. E. Fluctuations in Precambrian atmospheric oxygenation recorded by chromium isotopes. *Nature* **461,** 250–253 (2009).
13. Schröder, S., Lacassie, J. P. & Beukes, N. J. Stratigraphic and geochemical framework of the Agouron drill cores, Transvaal Supergroup (Neoarchean–Paleoproterozoic, South Africa). *S. Afr. J. Geol.* **109,** 23–54 (2006).
14. Knoll, A. H. & Beukes, N. J. Introduction: Initial investigations of a Neoarchean shelf margin-basin transition (Transvaal Supergroup, South Africa). *Precambr. Res.* **169,** 1–14 (2009).
15. Morris, A. W. Dissolved molybdenum and vanadium in the northeast Atlantic Ocean. *Deep-Sea Res.* **22,** 49–54 (1975).
16. Collier, R. W. Molybdenum in the Northeast Pacific Ocean. *Limnol. Oceanogr.* **30,** 1351–1354 (1985).
17. Anbar, A. D., Creaser, R. A., Papanastassiou, D. A. & Wasserburg, G. J. Rhenium in seawater: Confirmation of generally conservative behaviour. *Geochim. Cosmochim. Acta* **56,** 4099–4103 (1992).
18. Colodner, D. *et al.* The geochemical cycle of rhenium: A reconnaissance. *Earth Planet. Sci. Lett.* **117,** 205–221 (1993).
19. Morford, J. L. & Emerson, S. R. The geochemistry of redox sensitive trace metals in sediments. *Geochim. Cosmochim. Acta* **63,** 1735–1750 (1999).
20. Sundby, B., Martinez, P. & Gobeil, C. Comparative geochemistry of cadmium, rhenium, uranium, and molybdenum in continental margin sediments. *Geochim. Cosmochim. Acta* **68,** 2485–2493 (2004).
21. Yamashita, Y. *et al.* Comparison of reductive accumulation of Re and Os in seawater-sediment systems. *Geochim. Cosmochim. Acta* **71,** 3458–3475 (2007).
22. Erickson, B. E. & Helz, G. R. Molybdenum (VI) speciation in sulfidic waters: Stability and lability of thiomolybdates. *Geochim. Cosmochim. Acta* **64,** 1149–1158 (2000).
23. Zheng, Y., Anderson, R. F., Van Geen, A. & Kuwabara, J. Authigenic molybdenum formation in marine sediments: A link to pore water sulfide in the Santa Barbara Basin. *Geochim. Cosmochim. Acta* **64,** 4165–4178 (2000).
24. Algeo, T. J. & Lyons, T. W. Mo—total organic carbon covariation in modern anoxic marine environments: Implications for analysis of paleoredox and paleohydrographic conditions. *Paleoceanography* **21,** PA1016 (2006).
25. Crusius, J., Calvert, S., Pedersen, T. & Sage, D. Rhenium and molybdenum enrichments in sediments as indicators of oxic, suboxic and sulfidic conditions of deposition. *Earth Planet. Sci. Lett.* **145,** 65–78 (1996).
26. Cohen, A. S., Coe, A. L., Bartlett, J. M. & Hawkesworth, C. J. Precise Re–Os ages of organic-rich mudrocks and the Os isotope composition of Jurassic seawater. *Earth Planet. Sci. Lett.* **167,** 159–173 (1999).
27. Scott, C. *et al.* Tracing the stepwise oxygenation of the Proterozoic ocean. *Nature* **452,** 456–459 (2008).
28. Morford, J. L., Emerson, S. R., Breckel, E. J. & Kim, S. H. Diagenesis of oxyanions (V, U, Re, and Mo) in pore waters and sediments from a continental margin. *Geochim. Cosmochim. Acta* **69,** 5021–5032 (2005).
29. Raiswell, R. & Canfield, D. E. Sources of iron for pyrite formation in marine sediments. *Am. J. Sci.* **298,** 219–245 (1998).
30. Raiswell, R., Newton, R. & Wignall, P. B. An indicator of water-column anoxia: Resolution of biofacies variations in the Kimmeridge Clay (Upper Jurassic, UK). *J. Sedim. Res.* **71,** 286–294 (2001).
31. Poulton, S. W. & Raiswell, R. The low-temperature geochemical cycle of iron: From continental fluxes to marine sediment deposition. *Am. J. Sci.* **302,** 774–805 (2002).
32. Beukes, N. J. Facies relations, depositional environments and diagenesis in a major Early Proterozoic stromatolitic carbonate platform to basinal sequence, Campbellrand Subgroup, Transvaal Supergroup, southern Africa. *Sediment. Geol.* **54,** 1–46 (1987).
33. Sumner, D. Y. & Beukes, N. J. Sequence stratigraphic development of the Neoarchean Transvaal carbonate platform, Kaapvaal Craton, South Africa. *S. Afr. J. Geol.* **109,** 11–22 (2006).
34. Beukes, N. J. & Gutzmer, J. in *Banded Iron Formation-related High-Grade Iron Ore* Vol. 15 (eds Hagemann, S., Rosiere, C., Gutzmer, J. & Beukes, N. J.) 5–47 (Soc. Econ. Geol., Rev. Econ. Geol., 2008).
35. Altermann, W. & Nelson, D. R. Sedimentation rates, basin analysis and regional correlations of three Neoarchaean and Palaeoproterozoic sub-basins of the Kaapvaal Craton as inferred from precise U–Pb zircon ages from volcaniclastic sediments. *Sediment. Geol.* **120,** 225–256 (1998).
36. Pickard, A. L. SHRIMP U–Pb zircon ages for the Palaeoproterozoic Kuruman Iron Formation, Northern Cape Province, South Africa: Evidence for simultaneous BIF deposition on Kaapvaal and Pilbara Cratons. *Precambr. Res.* **125,** 275–315 (2003).
37. Bekker, A. *et al.* Dating the rise of atmospheric oxygen. *Nature* **427,** 117–120 (2004).
38. Guo, Q. *et al.* Reconstructing Earth's surface oxidation across the Archean-Proterozoic transition. *Geology* **37,** 399–402 (2009).
39. Poulton, S. W., Fralick, P. W. & Canfield, D. E. The transition to a sulphidic ocean ~1.84 billion years ago. *Nature* **431,** 173–177 (2004).
40. Klein, C. & Beukes, N. J. Geochemistry and sedimentology of a facies transition from limestone to iron-formation deposition in the Early Proterozoic Transvaal Supergroup, South Africa. *Econ. Geol.* **84,** 1733–1774 (1989).
41. Lyons, T. W. & Severmann, S. A critical look at iron paleoredox proxies: New insights from modern euxinic marine basins. *Geochim. Cosmochim. Acta* **70,** 5698–5722 (2006).
42. Li, C. *et al.* A stratified redox model for the Ediacaran ocean. *Science* **328,** 80–83 (2010).
43. Rooney, A. D., Selby, D., Houzay, J-P. & Renne, P. R. Re–Os geochronology of a Mesoproterozoic sedimentary succession, Taoudeni Basin, Mauritania: Implications for basin-wide correlations and Re–Os organic-rich sediments systematics. *Earth Planet. Sci. Lett.* **289,** 486–496 (2010).
44. Pavlov, A. A. & Kasting, J. F. Mass-independent fractionation of sulfur isotopes in Archean sediments: Strong evidence for an anoxic Archean atmosphere. *Astrobiology* **2,** 27–41 (2002).
45. Farquhar, J. & Wing, B. A. Multiple sulfur isotopes and the evolution of the atmosphere. *Earth Planet. Sci. Lett.* **213,** 1–13 (2003).
46. Ono, S. *et al.* New insights into Archean sulfur cycle from mass-independent sulfur isotope records from the Hamersley Basin, Australia. *Earth Planet. Sci. Lett.* **213,** 15–30 (2003).
47. Ono, S. *et al.* Lithofacies control on multiple-sulfur isotope records and Neoarchean sulfur cycles. *Precambr. Res.* **169,** 58–67 (2009).
48. Sverjensky, D. A., Lee, N. & Hazen, R. M. Weathering in the Late Archean and perturbations by oxygenic photosynthesis. *Eos Trans. AGU (Fall Meeting Suppl.)* **90,** Abstr. B12A-02 (2009).
49. de Kock, M. O., Evans, D. A. D. & Beukes, N. J. Validating the existence of Vaalbara in the Neoarchean. *Precambr. Res.* **174,** 145–154 (2009).
50. Simonson, B. M. *et al.* Correlating multiple Neoarchean–Paleoproterozoic impact spherule layers between South Africa and Western Australia. *Precambr. Res.* **169,** 100–111 (2009).


## Acknowledgements

We thank J. Kirschvink, J. Grotzinger, A. Knoll and the Agouron Institute for spearheading and funding the Agouron drilling project. This study was financially supported by the NASA Exobiology Program and the NASA Astrobiology Institute. B.K. was financially supported by an Agouron Institute Geobiology Fellowship. The NSF (Geobiology and Low Temperature Geochemistry and Sedimentary Geology and Paleontology programs) supported analytical work at the University of Maryland. The DFG supported measurements by A.J.K. at the University of Maryland while on sabbatical. S.W.P. acknowledges support from a NERC Research Fellowship. T. Algeo provided valuable insights that improved the manuscript. G. Arnold and D. Sumner are thanked for discussions. J. Kirschvink is thanked for access to samples. G. Arnold, I. Hilburn and T. Raub assisted with sample collection and preparation. G. Gordon provided analytical support.

## Author contributions

The research was planned by B.K., A.D.A., T.W.L. and A.J.K. Analytical protocols and data processing were carried out by B.K., C.T.R., A.J.K. and S.W.P. Manuscript preparation was spearheaded by B.K. with important contributions from all co-authors.

## Additional information

The authors declare no competing financial interests. Supplementary information accompanies this paper on www.nature.com/naturegeoscience. Reprints and permissions information is available online at http://npg.nature.com/reprintsandpermissions. Correspondence and requests for materials should be addressed to B.K.